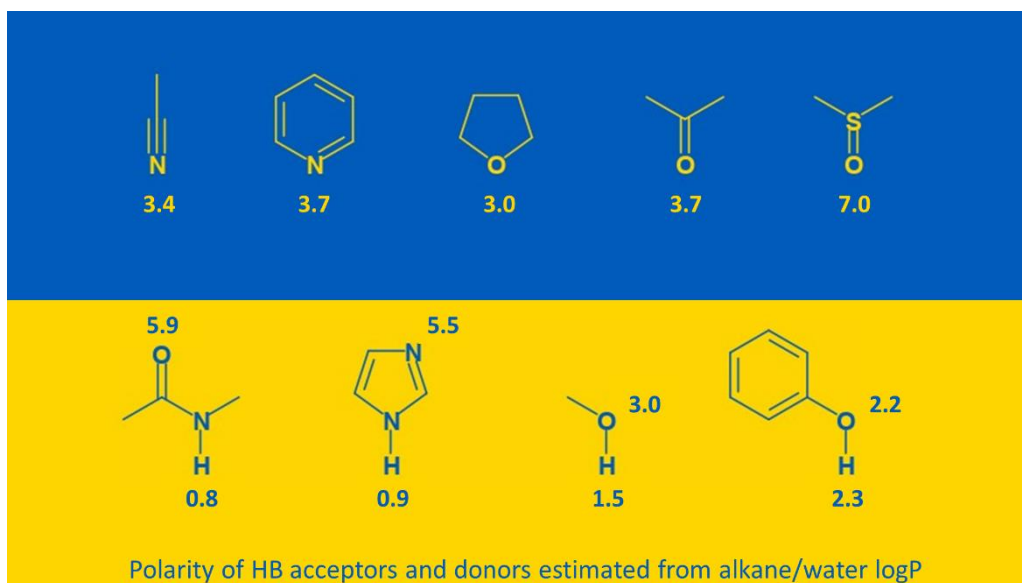


Hydrogen bond donors in drug design

Peter W. Kenny*

Berwick-on-Sea, North Coast Road, Blanchisseuse, Saint George, Trinidad and Tobago

ABSTRACT



In medicinal chemistry, hydrogen bond donors are seen to cause more problems than hydrogen bond acceptors and this study examines hydrogen bond donor-acceptor asymmetries in the context of drug design. Hydrogen bond acidity is reviewed and it is shown how polarity can be estimated for individual hydrogen bond donors and acceptors from alkane/water partition coefficient measurements. Hydrogen bond donors are generally less polar than hydrogen bond acceptors and desolvation penalty is therefore an implausible explanation for deleterious effects of hydrogen bond donors. Generally, the number of hydrogen bond acceptors in organic compounds exceeds the number of hydrogen bond donors and the apparently greater restrictiveness of the Rule of 5 for hydrogen bond donors may simply be a reflection of this imbalance. The weaker hydration of hydrogen bond donors implies that attempts to address polarity surfeit in optimization of permeability should be focused on hydrogen bond acceptors. Elimination of redundant hydrogen bond donors can potentially reduce active efflux and destabilize the solid state without resulting in unacceptable increases in lipophilicity. The key hydrogen bond donor-acceptor asymmetry in the context of target recognition is that the presence of a hydrogen bond donor usually implies that a hydrogen bond acceptor is also

present. Target-ligand hydrogen bonds form in aqueous media and design opportunities presented by frustrated hydration and secondary interactions are discussed. Hydrogen bond donors based on oxygen, nitrogen and carbon are compared as target recognition elements and potential benefits of halogen and chalcogen bond donors as replacements for hydrogen bond donors are discussed.

INTRODUCTION

“Five hydrogen bond donors, Dr. Worthing, may be regarded as a misfortune; to have ten looks like carelessness.”

With apologies to Oscar Wilde

Molecular recognition [1] provides a conceptual framework for drug design and many medicinal chemists consider molecular interactions [2–5] in design. Hydrogen bonding [6–12] is a key element of molecular recognition and is implicated in physicochemical phenomena such as DNA base-pairing, enzymatic catalysis [13], host-guest complex formation [14] and solid state stabilization [15, 16]. The cohesiveness of liquid water that forms the basis of the hydrophobic effect [17] is a consequence of strong, cooperative hydrogen bonds (HBs) between water molecules.

Hydrogen bonding stabilizes three-dimensional structures of drug targets, such as proteins and RNA [18], and is also an important determinant of binding affinity of drugs for their targets and anti-targets. However, the importance of individual ligand-target HBs cannot be inferred simply from inspection of the structure of a target-ligand complex since the contribution of an intermolecular contact to affinity is generally not an experimental observable [19]. Furthermore, drugs associate with their targets in aqueous environments which means that binding should be considered as an ‘exchange reaction’ [20]. This point is well made by Shen et al [21]:

“Molecular binding in an aqueous solvent can be usefully viewed not as an association reaction, in which only new intermolecular interactions are introduced between receptor and ligand, but rather as an exchange reaction in which some receptor–solvent and ligand–solvent interactions present in the unbound state are lost to accommodate the gain of receptor–ligand interactions in the bound complex.”

When interpreting structures of target-ligand complexes it is also important to be aware that contact between polar and non-polar atoms can destabilize a complex without being inherently repulsive [5, 22].

Hydrogen bonding also influences the absorption, distribution, metabolism and excretion (ADME) of drugs. The ease with which a drug can be transferred from water to a non-polar environment reflects the strength of the HBs that its molecules make with water and strongly influences both passive permeability and in vivo distribution. For the neutral form of a drug to

have good aqueous solubility, the HBs that its molecules make with water need to be energetically more favorable than the hydrogen bonds between its molecules in the solid state. One significant challenge in drug design is that intracellular unbound concentration [23, 24] cannot generally be measured for drugs in vivo.

Elimination of non-essential HBDs has been used as a medicinal chemistry tactic, for example in the design of the SARS-CoV-2 main protease inhibitor nirmatrelvir [25], and there is a commonly held view that HBDs are more detrimental than HBAs from the perspective of controlling exposure for orally dosed agents [26]:

“Of the guidelines suggested by Lipinski, hydrogen bond acceptors (HBAs) appear to be the least important and instead hydrogen bond donors (HBDs) are often the enemy of medicinal chemists. Particularly for compounds in the upper end of the molecular weight property range, HBDs can lead to very poor solubility, permeability and bioavailability. In contrast, compounds containing only HBAs, with no formal donor groups, can maintain good permeability and, therefore, bioavailability and blood–brain barrier penetration.”

Establishing definitively that HBDs do indeed cause more problems than HBAs for medicinal chemists is not a trivial exercise. Correlation does not constitute causation and, for example, it would be unwise to infer a causal relationship between donation of HBs and glucuronidation [27] of phenols. The number of HBDs (N_{HBD}) cannot generally be varied independently of the number of HBAs (N_{HBA}), making it difficult to deconvolute the effects of the two factors. In cheminformatic data analysis, it is essential to properly account for relationships between descriptors, such as that between the presence of an amine nitrogen in and the fraction (F_{sp^3}) of carbon atoms in the molecular structure that are tetrahedral [28].

Mobley et al [29] reported charge asymmetries for implicit solvent models and there are analogous HB donor-acceptor asymmetries in drug design. First, N_{HBA} tends to exceed N_{HBD} in molecular structures of interest to designers and this has particular relevance to stability of the solid state. Second, HBDs tend to be less strongly hydrated than HBAs and desolvation penalty is therefore not a plausible explanation for any ADME liability that might be linked to the presence of HBDs. Third, the presence of an HBD in a ligand structure generally implies that an HBA, which can be described as ‘co-occurring’, is also present and this usually needs to be considered when optimizing affinity.

This study is not intended as a comprehensive review and its focus is on energetic, rather than geometric, aspects of HB donation in the context of drug design. The study provides an

overview of HB acidity and shows how polarity contributions of individual HBDs and HBAs can be derived from partition coefficient measurements. The greater restrictiveness of the Rule of 5 (Ro5) for HBDs in comparison with HBAs is examined and the differing roles of HBDs and HBAs as determinants of permeability and aqueous solubility are discussed. Different types of HBD are compared as target recognition elements.

HYDROGEN BOND ACIDITY

HB acidity and basicity are usually quantified by measuring association constants [30] for formation of 1:1 hydrogen-bonded complexes in solvents such as 1,1,1-trichloromethane [9], tetrachloromethane [11] or cyclohexane [31] that lack hydrogen bonding capability. The concentration of a 1:1 complex cannot generally be measured in the presence of other 1:1 complexes and it is therefore necessary to use structurally-prototypical compounds, each with either a single HBA or HBD in these studies. HB acidity can be quantified by the association constant for formation of a 1:1 complex between a probe compound incorporating the HBD of interest and a reference compound with a single HBA such as N-methylpyrrolidinone [32], triphenylphosphine oxide [33] or pyridine N-oxide [31]. HB acidity can also be assessed spectroscopically using the shift in a carbonyl stretching frequency [9, 34] or from the difference in the ^1H NMR chemical shift of a protic hydrogen between dimethylsulfoxide and chloroform [35].

Measured values of HB acidity have been reported in a number of studies [9, 32–34, 36–41] although the body of published data is less extensive than for HB basicity on account of the greater structural diversity of HBAs. Association constants can be transformed [10, 42] to allow aggregation of data measured using different reference HBAs and illustrative values of α_2^{H} are given in Table 1. If data availability permits it may be preferable to compare HB acidity values that have all been measured using the same reference HBA and solvent. Scheme 1 shows how HB acidity, quantified as $(\log K_a)$ [9, 34], can be modulated by substitution even when the effects of substituents are relayed from an aromatic ring to a hydroxyl group by an amidic NH (Scheme 1C).

Table 1. Measured hydrogen bond acidity

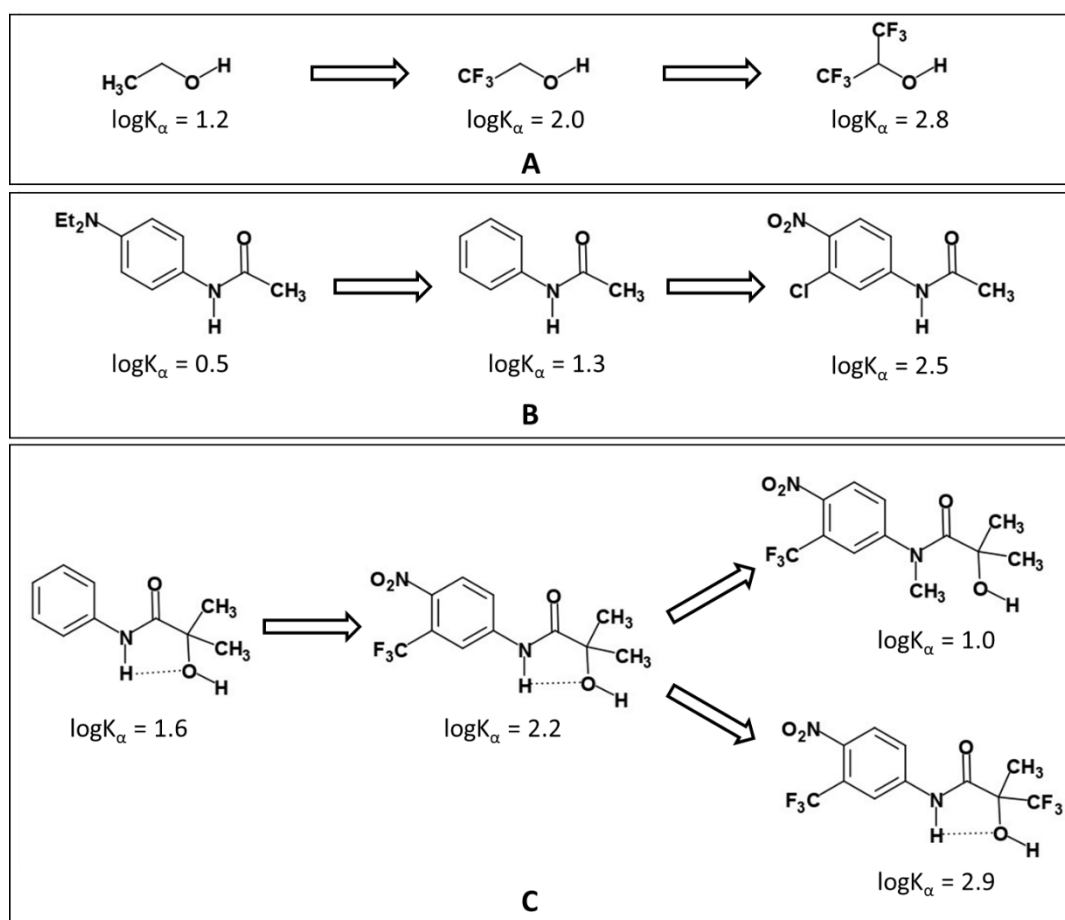
Hydrogen bond donor	Type	$\alpha_2^{\text{H a}}$
Water	OH ₂	0.35 ^b
Methanol	OH	0.37
Ethanol	OH	0.33
2,2,2-Trifluoroethanol	OH	0.57
1,1,1,3,3,3-Hexafluoropropan-2-ol	OH	0.77
Perfluoro-t-butanol	OH	0.86
Phenol	OH	0.60
2-Chlorophenol	OH	0.66 ^c
2,6-Dichlorophenol	OH	0.42 ^c
3-Methylphenol	OH	0.58 ^c
3-Chlorophenol	OH	0.69 ^c
4-Chlorophenol	OH	0.67
4-Trifluorophenol	OH	0.75 ^c
4-Methoxyphenol	OH	0.63 ^c
4-Nitrophenol	OH	0.82
Acetic acid	OH	0.55
Trifluoroacetic acid	OH	0.95
Acetone oxime	OH	0.43 ^d
Aniline	NH ₂	0.26 ^b
4-Nitro-N-methylaniline	NH	0.37 ^e
N-Methylacetamide	NH	0.38
Trifluoroacetamide	NH ₂	0.51 ^e
Acetanilide	NH	0.48 ^e
4-Diethylaminoacetanilide	NH	0.32 ^e
3-Chloro-4-nitroacetanilide	NH	0.69 ^e
Thioacetanilide	NH	0.51 ^e
Succinimide	NH	0.49 ^f
Tetrafluorosuccinimide	NH	0.89 ^f
Bistrifluoroacetamide	NH	0.71 ^e
4-Methylbenzenesulfonamide	NH ₂	0.44 ^e
N-Benzyl-4-methylbenzenesulfonamide	NH	0.40 ^e
Pyrrole	NH	0.41
Indole	NH	0.44 ^c
2-(3-Benzoyloxypropyl)-imidazole	NH	0.45 ^c
4-Methylthio-1,2,3-triazole	NH	0.60 ^c
3-(3-Phenylpropyl)-1,2,4-triazole	NH	0.63 ^c
Dichloromethane	CH ₂	0.13 ^b
Trichloromethane	CH	0.20
1-Heptyne	CH	0.13
3,3,3-Trifluoroprop-1-yne	CH	0.28 ^g
Cyanoacetylene	CH	0.36 ^g

^a Taken from [36] unless stated otherwise ^b Not corrected for number of donor hydrogen atoms ^c Obtained by applying equation 10 [39] to $\log K_a$ value reported in [9] ^d From [41] ^e From [39] ^f From [38] ^g From [33]

The correlations between HB acidity and the acid dissociation constant ($\text{p}K_a$) are typically stronger within structural classes (see Figure 5 in [9]) than for structurally-diverse HBDs. Although phenol ($\text{p}K_a = 10.0$; $\alpha_2^{\text{H}} = 0.60$; $\log K_a = 2.14$) is a significantly weaker acid than acetic acid ($\text{p}K_a = 4.8$; $\alpha_2^{\text{H}} = 0.55$; $\log K_a = 2.04$) it is slightly stronger HB donor [9]. This observation can be explained by a repulsive secondary interaction [43] between the *syn* lone pair of the carbonyl oxygen and any HBA that accepts an HB from the carboxylic acid. The

greater HB acidity of N,N'-dicyclohexylurea relative to amides that is inferred from the shift in carbonyl stretching frequency is likely to be due to bifurcated HB donation to the carbonyl oxygen of N-methyl pyrrolidone which was used as a reference HBA in the study [9].

The HB acidity values measured for structurally prototypical compounds can often be used to predict HB acidity for compounds that are structurally more complex. Hydrogen bonding has a large electrostatic component and predictive models based on calculated molecular electrostatic potential (MEP) [2, 40, 44, 45] can be used when relevant HB acidity measurements are not available. Models for HB acidity based on MEP enable contributions of non-equivalent HBDs (e.g., amide NH₂) to a measured value to be deconvoluted [45]. Designers should also be aware of the diiodine basicity scale [46] since halogen bond [47] donors can be used to mimic HBDs.



Scheme 1. Effects of structural modification on hydrogen bond acidity. Reference $\log K_\alpha$ values for t-butanol (0.8), phenol (2.1), 4-nitrophenol (3.1), N-hexylheptamide (0.6), bistrifluoroacetamide (2.6), 4-methylbenzenesulfonamide (1.1), indole (1.1) and data shown in panels A/B are from [9]; data shown in panel C are from [34]

PARTITION COEFFICIENTS

Knowledge of HB acidity can be used to assess solvation potential for individual HBDs but cannot be used to make comparisons between HBDs and HBAs. One approach to making such comparisons is to analyze partition coefficient measurements for structurally-prototypical model compounds [48].

Although the 1-octanol/water partition coefficient ($\log P_{\text{oct}}$) [49–51] is a widely used design parameter in medicinal chemistry, it is unsuitable for characterization of aqueous solvation because 1-octanol can form HBs with solutes and $\log P_{\text{oct}}$ does not sense HBDs in molecular structures [52, 53]. The alkane/water partition coefficient ($\log P_{\text{alk}}$) [54–66] is actually more suitable for assessing contributions of HBAs and HBDs to aqueous solvation. Water content at saturation for cyclohexane and hexadecane, the most commonly used solvents for $\log P_{\text{alk}}$ measurement, is much lower than that of 1-octanol [67] and partitioning [68, 69] of charged forms of solutes into the organic solvent is also less of a concern than for 1-octanol. A saturated hydrocarbon is actually a more appropriate reference than gas phase for modelling contact between polar ligand atoms and non-polar target atoms since contributions of van der Waals dispersion forces [5] are better accounted for. Furthermore, $\log P_{\text{alk}}$ is also more easily measured than free energy for transfer from gas phase to water [70].

The $\text{Clog}P_{\text{alk}}$ model [67] provides a framework in which the individual contributions of HBAs and HBDs to aqueous solvation can be assessed and this study uses the parameters from Version 2.0 of the model [48]. The basis for this model is the strong linear relationship between $\log P_{\text{alk}}$ and calculated molecular surface area (MSA) observed for saturated hydrocarbon solutes and an analogous approach based on molecular volume has previously been reported [71]. The $\text{Clog}P_{\text{alk}}$ model defines polarity, Q , for a compound as the difference between the $\log P_{\text{alk}}$ value calculated for a hypothetical, saturated hydrocarbon with the same MSA and the measured value [48]:

$$Q = 0.0338 \times (\text{MSA}/\text{\AA}^2) - 0.284 - \log P_{\text{alk}} \quad (1)$$

The parameters in the $\text{Clog}P_{\text{alk}}$ model are fragment-based contributions, q_i that are defined by substructure and polarity is calculated as a sum of the parameters [48]:

$$Q = \sum_i q_i \quad (2)$$

The ClogP_{alk} model decomposes logP_{alk} into a molecular size term and a polarity term. Partition coefficients measured using 1-octanol or other solvents could easily be decomposed in a similar manner which might reduce descriptor redundancy in analyses of drug-likeness. Polarity as defined by the ClogP_{alk} model is a difference between two logP_{alk} values and is therefore invariant with respect to change in standard state definition.

Table 2: Polarity of HB acceptors

Substructure	q ^a	pK _{BHX} ^c
Benzene	1.0	-0.49
N,N-Dialkylaniline	2.7 ^b	0.39
1-Methylpyrrole		0.23
1-Alkylindole	2.5	
Aliphatic tertiary amine	3.8	1.98 (triethylamine)
		2.11 (N-methylpiperidine)
		2.71 (quinuclidine)
Pyridine	3.7	1.86
1-Alkylimidazole	5.5	2.72
Alkyl nitrile	3.4	0.91
Dialkyl ether	3.0	1.01 (diethyl ether)
		1.36 (oxetane)
		1.28 (tetrahydrofuran)
Alkyl-aryl ether	2.2	0.09 (anisole) ^d
Dialkyl ketone	3.7	1.18 (acetone)
		1.39 (cyclohexanone)
Dialkyl ester	3.5	1.00
Trialkyl tertiary amide	5.9	2.44
Dialkyl sulfone	6.0	1.40
Dialkyl sulfoxide	7.0	2.54 ^e

^a See ClogPalk.param.2.0 (parameters) and ClogPalk.vbind.2.0 (vector bindings for SMARTS definitions) and text files in supplemental information for [48] in order to obtain q value corresponding to substructure by multiplying number of non-hydrogen atoms in SMARTS by slope parameter. ^b Calculated from MSA (154 Å²) and hexadecane/water logP (2.2) [59] for N,N-dimethylaniline using eqn (1). ^c Measured pK_{BHX} values from [72] and unless stated otherwise, measured values corresponding to alkyl substructures are for methyl derivatives. ^d From [73]. ^e Not corrected for number of HBA atoms.

The polarity from a measured logP_{alk} value can be meaningfully assigned to a particular HBA if no HBDs (or other non-equivalent HBAs) are present in the molecular structure. A number of illustrative polarity values are presented for structurally prototypical compounds in Table 2. The high polarity of amides and sulfoxides is partly due to oxygen having two lone pairs since measured pK_{BHX} values [72] indicate that N-methylimidazole (2.72) is actually a stronger HBA than either N-methylpyrrolidinone (2.38) or dimethylsulfoxide (2.54). Given the polarity of benzene, one might speculate that the observed polarity of pyridine is partly due to its π-system. However, this is likely to be less significant than for benzene because nitrogen draws electron density out of the π-cloud and donation of an HB by water to nitrogen will further strengthen this effect.

Polarity values for HBDs cannot be directly derived because HBDs are never present in molecular structures in the absence of HBAs. The π -system of indole, which lacks a conventional HBA, still makes a substantial contribution to polarity (in contrast to pyridine, HB donation by the indole NH would be expected to lead to an increase in the HB basicity of the π -system). Nevertheless, polarity can be estimated for an HBD if measured $\log P_{\text{alk}}$ is available for appropriate model compounds and this is also the basis for the $\text{ClogP}_{\text{alk}}$ parameterization [48]. For example, an estimate (0.8) for the polarity of secondary amide NH can be derived by comparing q values for secondary and tertiary aliphatic amides. Polarity values derived from the $\text{ClogP}_{\text{alk}}$ parameterization [48] and measured values of HB acidity ($\log K_a$) are presented for a number of HBDs in Table 3.

Table 3. Polarity of hydrogen bond donors

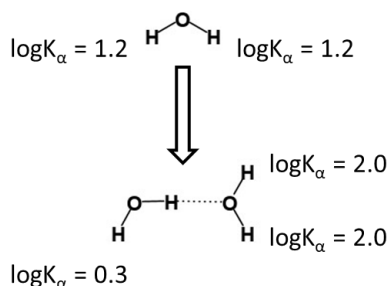
HBD	q^a	$\alpha_2^{\text{H}^c}$
Aniline	1.1 ^b	0.26 ^d
Acyclic secondary amide	0.8	0.38
Primary amide	1.3	
Cyclic imide	1.3	0.50
Primary sulfonamide	1.9	0.44 ^d
Indole	1.0	0.44
Imidazole	0.9	0.45 ^e
Aliphatic alcohol	1.5	0.33
Phenol	2.3	0.58
Aliphatic carboxylic acid	2.1	0.55

^a See *ClogPalk.param.2.0* (parameters) and *ClogPalk.vbind.2.0* (vector bindings for SMARTS definitions) text files in supplemental information for [48] in order to obtain q value corresponding to substructure by multiplying number of non-hydrogen atoms in SMARTS by slope parameter. ^b Subtract Q (2.7; Table 2) for dimethylaniline from Q (3.8) calculated for aniline using equation (1) with MSA (120 Å²) and hexadecane/water $\log P$ (-0.04) [59] for N,N-dimethylaniline. ^c From Table 1. ^d Value not normalized for number of hydrogen atoms in HBD substructure. ^e Value is for 2-(3-benzoyloxypropyl)-imidazole

With the exception of the alkyl-aryl ether oxygen which is a weak HBA (a pK_{BHX} value of 0.09 has been reported [73] for anisole) the heteroatom-based HBAs in Table 2 are all more polar than the HBDs in Table 2. The amide NH HBD appears to be comparable in polarity with benzene, which would not usually be counted as an HBA even though a pK_{BHX} value of -0.49 [72] has been measured for it. This HB donor-acceptor asymmetry is closely related to the charge asymmetries discussed by Mobley et al [29] and is largely a consequence of water being a better HBD than HBA. Phenols and carboxylic acids present the most polar HBDs but these are still much less polar than the HBAs of amides or sulfoxides.

The HB acidity of a hydroxyl group would be expected to increase when it accepts an HB just as just as its HB basicity would be expected to increase when it donates an HB. This

behavior, which is seen in MEP calculations [45, 63], indicates that the HBD and HBA of a hydroxyl group interact with water cooperatively. A portion of the polarity of a hydroxyl group cannot therefore be assigned exclusively to either its HBD or HBA and the q value derived for a hydroxylic HBD should therefore be regarded as an upper limit. The predicted $\log K_{\alpha}$ values [45] given in Scheme 2 illustrate how dimerization of water leads to an increase in the HB acidity of the water molecule that accepts the HB and a decrease in the HB acidity of the donor water molecule.



Scheme 2. HB acidity ($\log K_{\alpha}$) for water and its dimer predicted from calculated MEP using equation 3g (water is numbered 69) [45]. Reference $\log K_{\alpha}$ values for methanol (1.5), ethanol (1.2) and phenol (2.1) taken from [9].

Intramolecular HB formation profoundly affects physicochemical behavior of compounds such as cyclic peptides [74]. The insensitivity of $\log P_{\text{oct}}$ to HBDs [52, 53] suggests that $\log P_{\text{alk}}$ [62] should be more useful than $\log P_{\text{oct}}$ for studying intramolecular hydrogen bonding and toluene/water has also been proposed for this purpose [75]. The polarity values for the carbonyl oxygen (5.9) and NH (0.8) of an aliphatic secondary amide suggest that formation of an intramolecular HB in a cyclic peptide will lead to a 6.7 log unit reduction in polarity. This figure should be taken as an upper limit that only applies when the intramolecular HB persists in water and the amide carbonyl oxygen accepting the intramolecular HB is unable to accept an additional HB.

The polarity of an individual HBA or HBD quantifies the cost of bringing it into contact with a non-polar region of a molecular surface. Polarity values derived from measured $\log P_{\text{alk}}$ suggest that unsatisfied hydrogen bonding capacity will usually have a less deleterious effect on stability for HBDs than for HBAs. This suggests that scoring functions used in virtual screening should penalize contact between polar and non-polar atoms at the ligand-target interface to a lesser extent for HBDs than for HBAs. The q values derived from measured $\log P_{\text{alk}}$ measurements for individual HBDs and HBAs could even be used to set the penalties.

Conformations of molecules are similarly destabilized in water by contact between polar and non-polar atoms and less destabilization should be anticipated for HBDs than for HBAs.

The polarity values for the secondary amide NH (0.8) and carbonyl oxygen (5.9) derived from $\log P_{\text{alk}}$ measurements are consistent with the observation that, for high resolution protein structures, “9.5% and 5.1% of buried main-chain nitrogen and oxygen atoms, respectively, fail to hydrogen bond under our standard criteria, representing 5.8% and 2.1% of all main-chain nitrogen and oxygen atoms” [76]. The large difference in desolvation cost between the HBD and HBA of a secondary amide is a factor which could be taken account of when modelling polypeptide chains.

THE RULE OF 5

Most drug discovery scientists are familiar with Ro5 [77] and compliance is sometimes taken as an indication that a compound is drug-like. The ‘drugs’ in the data set used to derive Ro5 were selected on the basis of having been taken into a phase 2 clinical trial at some point before Ro5 was published in 1997. Although the focus of Ro5 is oral absorption, clinical candidates may fail to progress to phase 2 trials for reasons other than being poorly absorbed. Bioavailability reflects first pass metabolism as well as oral absorption, hydroxyl groups are prone to glucuronidation [27] and anilines may be metabolically activated to toxic entities [78].

Ro5 is framed in terms of lipophilicity, molecular size and polarity (as quantified by N_{HBA} and N_{HBD}) and compliance with Ro5 requires that $N_{\text{HBA}} \leq 10$ and $N_{\text{HBD}} \leq 5$. Although Ro5 raised awareness of molecular size and lipophilicity as risk factors in drug design, it is too blunt an instrument to be of practical utility in lead optimization. Examination of percentiles in physicochemical property distributions is an indirect way to study relationships between permeability or solubility and physicochemical properties and the same can be said of analyses of time-dependency [79, 80] of the distributions. The indirect nature of these approaches to data analysis means makes them unsuitable for deconvoluting effects of HBAs and HBDs, even when relationships between physicochemical properties are properly accounted for. It is significant that attempts to build global models for permeability and solubility, using only the dimensions of the chemical space in which Ro5 is specified as descriptors, do not appear to have been successful.

In determining compliance with Ro5 all nitrogen and oxygen atoms are counted as HBAs and any hydrogen atom bonded to an HBA contributes to the HBD count. The Ro5 specification of HBAs is excessively permissive in that amide and amide-like nitrogen atoms are counted as HBAs. This exaggerates a natural imbalance between N_{HBA} and N_{HBD} in molecular structures of interest to designers. Although Shultz [80] correctly notes that “*not a single FDA approved oral drug has more HBD than HBA*”, this is largely a reflection of the overly permissive nature

of the Ro5 HBA specification. According to the Ro5 specifications, there are five HBAs and five HBDs in the molecular structure of metformin although three of the HBAs are amide-like nitrogen atoms which would not have been counted had more physically realistic definitions been used. It is likely that an intramolecular HB analogous to that observed in the crystal structure of biguanide [81] would persist in aqueous solution for the neutral form of metformin, leaving it with a single HBA and 4 HBDs.

The mean $N_{\text{HBD}}/N_{\text{HBA}}$ ratio for 749 FDA approved drugs in the data set provided by Shultz [80] is 0.34 with standard deviation of 0.25 and standard error in the mean of 0.01. This is significantly less than the ratio (0.5) of maximum N_{HBD} and N_{HBA} values permitted for compliance with Ro5. As such, Ro5 could actually be considered to be more permissive for HBDs than HBAs when the differing frequencies with which HBDs and HBAs occur in drug molecular structures are accounted for.

The differing acceptability thresholds for HBAs and HBDs in the Ro5 specification have resulted in surprisingly little discussion in the drug discovery literature. Neither the 2002 study by Veber et al [82] nor the 2004 study by Vieth et al [83] makes any suggestion that HBDs are any more deleterious than HBAs for oral bioavailability. Oprea [84] has invoked the lack of HBDs in lipid head groups while others have suggested that the acceptability thresholds may simply reflect the relative numbers of HBAs and HBDs occur in molecular structures of drugs [53]. The cutoffs used to apply Ro5 are intended to exclude 10% of the data although Shultz [80] has observed that 5% of oral drugs have more than 5 HBDs while 7% have more than 4 HBDs. Desolvation penalty is not a plausible explanation for the greater restrictiveness of Ro5 for HBDs because HBAs are typically more strongly solvated than HBDs.

Raschka et al [85] argue that protein-ligand interfaces are ‘polarized’ in that there is “*a strong trend for intermolecular hydrogen bonds to favor donors on the protein side*”. Given that N_{HBA} typically exceeds N_{HBD} for ligands, this observation is unsurprising since favoring HBAs on the protein side would reduce the chances of forming HBs at the interface while increasing risk of contact between HBAs and non-polar atoms. The view that polarization of binding interfaces is imposed by the HBA/HBD balance of the ligand is supported by the observation [85] that binding sites for peptide ligands ($N_{\text{HBA}} = N_{\text{HBD}}$ for peptide backbones) “*showed no strong preference for donating versus accepting H-bonds*”.

PERMEABILITY

Designers usually need to consider permeability since drugs must pass through cell membranes in order to be orally absorbed [86] (at least by the transcellular route) and to engage intracellular

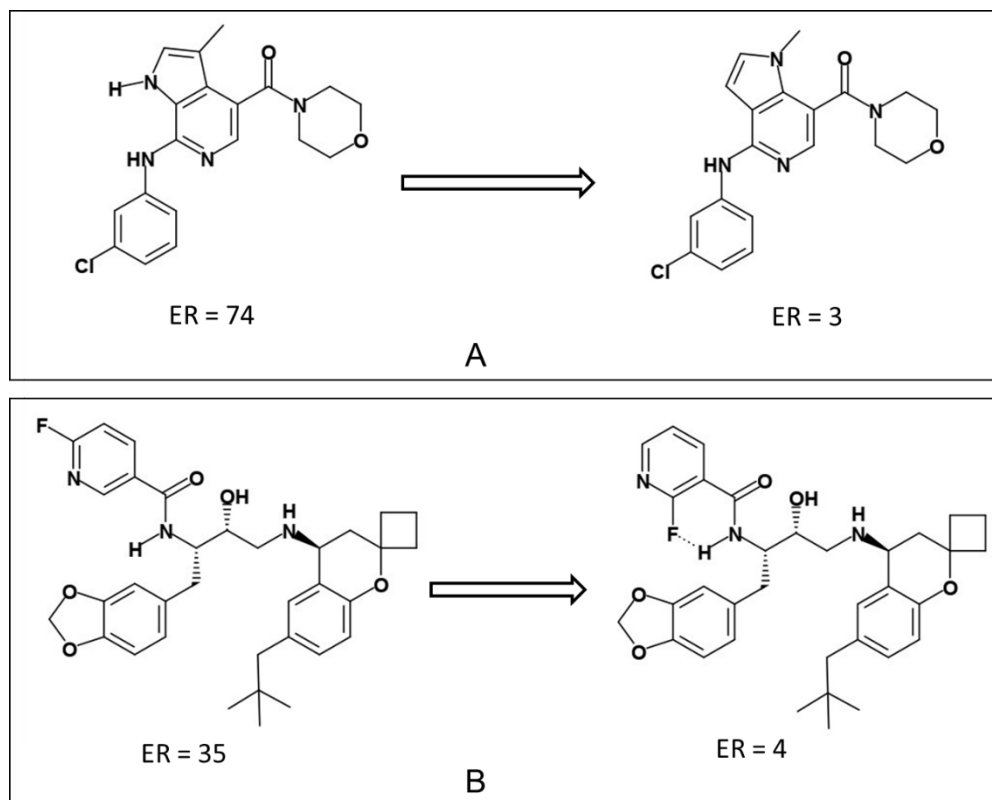
targets [24]. Bacterial cell envelopes, biofilms and intracellular pathogens present additional permeability challenges. For neutral drugs, poor permeability typically results either from a surfeit of polarity or from active efflux, although intestinal absorption of an orally-dosed drug may also be limited by solubility and dissolution rate. Although cell-free permeation assays [87, 88] have the advantages of being more robust than cell-based assays [89] and can typically be run at higher throughput, they provide no information about active efflux. When interpreting permeability measurements, it is important to be aware that assays have upper limits of quantitation.

The polarity estimates for HBAs and HBDs derived from $\log P_{\text{alk}}$ can be used to interpret the response of measured permeability to changes in N_{HBD} . For example, Klein et al [90] report that isosteric replacement of an amide with an ester leads to improved passive permeability for a series of targeted protein degraders. The data in Tables 2 and 3 suggest that this structural transformation will lead to a 3.2 log unit decrease in polarity (2.4 log unit from weakening the carbonyl oxygen HBA and 0.8 log unit from the elimination of the amidic HBD). A smaller polarity decrease (0.8 log unit) is predicted for N-methylation of the amide while reduction of the ester carbonyl to methylene would be expected to result in a further decrease in polarity of 0.5 log unit.

Permeability is a particularly important issue in treatment of central nervous system (CNS) disorders because drugs typically need to pass through the blood-brain barrier (BBB) [91] in order to engage targets and a number of methods can be used to measure BBB permeability [92, 93]. There is a consensus that control of polarity is critical if acceptable BBB permeability is to be achieved [91, 94] and PSA figures prominently in guidelines for achieving optimal brain exposure such as the central nervous system multiparameter optimization (CNS MPO) desirability tool [95]. A related polarity descriptor that has been proposed [96] as a predictor of brain exposure is the difference, $\Delta\log P$ [55], between $\log P_{\text{alk}}$ and $\log P_{\text{oct}}$ which quantifies hydrogen bonding capacity. There appears to be little direct evidence that HBDs compromise passive BBB permeability to a greater extent than HBAs.

Limited brain exposure resulting from active efflux [91, 97] is a common issue for CNS drug discovery programs. Hitchcock suggests “*a dominant role of tPSA and particularly HBD count on the average P-gp efflux ratio*” [97]. However, this observation should not be invoked as evidence that HBDs represent a greater liability than HBAs for active efflux since topological polar surface area (tPSA) is likely to be strongly correlated with N_{HBA} . This view is supported by the correlations between PSA and N_{HBA} reported by Veber et al ($r = 0.93$ for oral bioavailability data set; $r = 0.87$ for permeation data set) [82] and Vieth et al ($r = 0.96$)

[83]. It is also difficult to deconvolute the effects of N_{HBD} and N_{HBA} in data analysis because the two factors are likely to be correlated (Vieth et al [83] report a correlation for which $r = 0.78$) and cannot generally be varied independently of each other.



Scheme 3. Efflux ratio (ER) cliffs associated with elimination or masking of HBDs

A significant reduction in efflux ratio (ER) resulting from elimination or masking of an HBD can be interpreted as evidence that the HBD is an active efflux liability and two illustrative examples have been reviewed by Hitchcock [97]. The isosteric transformation in Scheme 3A eliminates an HBD and the resulting decrease in ER from 74 to 3 identifies the azaindole HBD as an active efflux liability [98]. The transformation in Scheme 3B masks the amidic HBD by moving a fluoro substituent from C2 of a pyridine ring to C6, leading to a decrease in ER from 35 to 4 [99]. The structurally conservative nature of these transformations increases confidence that the active efflux observed is actually due to HB donation by the HBD in each case.

The choice of tactics for dealing with poor permeability is dictated by whether permeability is limited by polarity or active efflux. In drug design, most of the polarity of compounds tends to be due to their HBAs and efforts to address polarity-limited passive permeability should therefore be focused on HBAs rather than HBDs. Elimination of redundant HBDs is an

appropriate tactic for optimizing permeability that is limited by active efflux since it would be expected to result in smaller increases in lipophilicity than elimination of HBAs.

AQUEOUS SOLUBILITY

Passive absorption of an orally-dosed drug is driven by the concentration gradient of its permeating form (usually assumed to be neutral for ionizable compounds) across the intestinal wall and drugs need to be adequately soluble in order to be well-absorbed. When designing drugs for oral dosing it is important to be aware that “*screening solubility in simple aqueous media tends to underpredict the solubilizing capacity of the intestinal environment for many lipophilic drugs and drug candidates*” [100]. Enhanced solubility in intestinal fluid is beneficial in that it maintains more of the dose in the liquid phase and the ionized form of a drug can potentially facilitate diffusion of the neutral form in aqueous phase. However, the free concentration of the neutral form of a drug in intestinal fluid is typically limited by its aqueous solubility and achieving good intrinsic solubility remains a valid design objective.

The intrinsic aqueous solubility of a compound is determined by the relative strengths of the interactions between its molecules in the solid state and the interactions that its molecules make with water. One tactic for addressing poor aqueous solubility is to increase polarity, either by linking polar atoms to the scaffold (adds molecular weight but synthesis tends to be easier) or by replacing non-polar atoms in the scaffold with polar atoms (synthesis is likely to be more difficult). However, increased polarity brings risks of reduced affinity for therapeutic target(s) and reduced permeability.

Alternatively, the designer can try to eliminate or weaken molecular interactions in the solid state, for example, by increasing the degree of imbalance between HBAs and HBDs. Drugs typically have fewer HBDs than HBAs [80] and Desiraju has noted that “*in small organic molecules the acceptors are generally in excess of the donors, and so ‘free’ X–H groups are extremely rare*” [16]. These observations suggest that HBDs, rather than HBAs, should be eliminated in order to engineer a greater imbalance between HBAs and HBDs. The ‘direction’ ($N_{\text{HBD}} < N_{\text{HBA}}$) of the imbalance is fortuitous because elimination of the less polar HBDs would also be expected to result in smaller losses of solvation energy. Consideration of molecular complexity [101] suggests that elimination of an HBD should increase the likelihood that the remaining HBDs will form HBs with optimal geometry. This implies that the destabilization of the solid state resulting from elimination of a single HBD is likely to increase as HBDs are progressively eliminated.

Analysis of the effects of N-methylation on aqueous solubility of amides illustrates how elimination of HBDs can be used to improve aqueous solubility [102]. The results of matched molecular pair analysis (MMPA) presented in Table 4 show that N-methylation of acyclic secondary amides derived from aliphatic amides tends to result in increased aqueous solubility. While this observation appeared counter-intuitive when originally made in 2003 for a small number of glycogen phosphorylase inhibitors from a single structural series, it is perhaps not too surprising given that HBDs are typically more numerous than HBAs in molecular structures of interest to designers and less strongly solvated. The results in Table 4 indicate that, for this class of amide, the effect of N-methylation on solid state stability tends, on average, to outweigh its effect on solvation.

Table 4. Matched molecular pair analysis of effect on aqueous solubility (S) of N-methylation of secondary amides

Amide class	Mean ^a	SD ^b	SE ^c	N ^d	%Increase ^e
Acyclic; aliphatic amine	0.59	0.71	0.07	109	76
Benzanilide	1.49	0.47	0.15	9	100
Cyclic	0.18	0.76	0.25	9	44

^a Mean value for $\log(S_{\text{NMe}}/S_{\text{NH}})$. ^b Standard deviation for $\log(S_{\text{NMe}}/S_{\text{NH}})$. ^c Mean value of $\log(S_{\text{NMe}}/S_{\text{NH}})$. ^d Number of $[\text{C}(=\text{O})\text{NH} \rightarrow \text{C}(=\text{O})\text{NMe}]$ matched molecular pairs. ^e Percentage of matched pairs for which N-methyl analog is more soluble

The effects of N-methylation on aqueous solubility vary considerably across the three classes of amide in Table 4 and this example highlights the importance of accounting for structural context in MMPA [102]. The results for benzanilides are particularly striking and reflect the inversion of the trans/cis conformational preference of acyclic secondary amides that results from N-methylation [103]. Aqueous solubility of cyclic amides appears less affected by N-methylation which probably reflects constraints imposed by the cyclic amide geometry making it difficult to form “*infinite ladders of hydrogen bonds*” [104] in the solid state. Cyclic amide geometry is more compatible with formation of hydrogen-bonded dimers with the two interfacial HBs in a six-membered ring. Although Etter’s rules do not explicitly apply to hydrogen-bonded dimers it is noteworthy that rule 2 states that “*six-membered-ring intramolecular hydrogen bonds form in preference to intermolecular hydrogen bonds*” [15].

It has been suggested that aromatic rings [105] and unsaturated carbon atoms [106] should be considered as design liabilities. Disruption of molecular planarity and symmetry [107] has been proposed as a tactic for improving aqueous solubility and replacement of a benzene linker with bicyclo[1.1.1]pentane or bicyclo[2.2.2]octane leads to increased solubility in water [108]. The ability of molecules to pack into a crystal lattice can plausibly be invoked to explain poor

aqueous solubility of compounds with planar and symmetrical molecular structures. However, packing ability becomes a much less convincing explanation for the effects of aromatic rings on aqueous solubility when molecular structures are neither planar nor symmetrical, as is the case for many drugs. One explanation is that atoms in aromatic rings make stronger interactions with HBAs, HBDs and atoms in other aromatic rings [109, 110] than do their saturated counterparts which can only interact by van der Waals dispersion forces. Alternatively, imbalance between HBAs and HBDs may increase the likelihood that aromatic CHs [111] interact with HBAs and similar reasoning can be used to explain the effects on aqueous solubility of halogen bond donors [47] such as bromine atoms [104].

HYDROGEN BOND DONORS AND TARGET RECOGNITION

A major focus of structure-based ligand design is to introduce and optimize interactions between polar atoms at target-ligand interfaces. The lower structural diversity of HBDs when compared with HBAs means that the range of options available for incorporation of HBDs in ligand structures is more restricted than for HBAs. The key HB donor-acceptor asymmetry when optimizing affinity is that the presence of an HBD (e.g., amide NH) in a molecular structure almost invariably implies the co-occurrence of an HBA (e.g., amide carbonyl oxygen). In contrast, an HBA such as pyridine nitrogen or sulfone oxygen can be present in a molecular structure without requiring co-occurrence of an HBD. The need to accommodate co-occurring HBAs constrains how HBDs can be positioned and this becomes particularly significant when targeting HBAs within narrow binding pockets.

Drugs associate with their targets in aqueous media and association should be seen as an exchange reaction [20, 21]. In gas phase, increased HB acidity or HB basicity for either of a pair of hydrogen-bonded atoms at a binding interface would generally be expected to lead to greater stabilization of the complex. In an aqueous environment, the extent to which a ligand-target HB stabilizes the complex is determined by how effectively the interacting HBD and HBA compensate each other for lost solvation. This suggests HB acidity/basicity of ligand HBDs/HBAs could be optimized [2, 45] for affinity just as ligand charge distributions can be optimized for affinity [21, 112].

The presence of water molecules at the target-ligand interface introduces an additional layer of complexity to structure-based ligand design [113] and there is considerable interest in characterization of water molecules in contact with targets [114–120]. A water molecule is expected to incur an entropic penalty [121] when it makes contact with the binding site of the target and an enthalpic penalty might also be anticipated when the contact is with a non-polar

region of the target molecular surface. One consequence of the weak HB basicity ($pK_{\text{BH}^+} = 0.65$) [72] of water is that designers have a wider range of options for displacing water molecules that accept HBs from targets than is the case for water molecules donating HBs to targets.

When polar atoms in a binding site are in close proximity, the water molecules in contact with them may be unable to simultaneously form HBs with optimal geometry [48] and hydration can be described as ‘frustrated’ [122, 123]. In these situations, interaction potential of polar atoms in a binding site may be more effectively satisfied by a complementary arrangement of polar atoms that is held in place by covalent bonds. When polar atoms in the binding site are in close proximity, it is likely that the polar atoms in the ligand that make contact with them will also be in close proximity. Frustration of binding site hydration therefore implies that hydration of a ligand that is complementary to the site is also likely to be frustrated. The extremely high affinity of streptavidin for biotin is of considerable interest [124, 125] in the molecular recognition field and frustration of hydration is likely to be a contributing factor since there are five HBs between the protein and the cyclic amide substructure of the ligand [126].

One might anticipate that frustration of hydration will be more pronounced when the water molecules are interacting with polar atoms of the same type (e.g., HBD). Alignment of HBDs or lone pairs is relevant to design [22] because it can lead to attractive secondary interactions [43] which tend to augment the effects of frustrated hydration (Figure 1). Lone pair alignment explains the stronger HB basicity of lactones relative to acyclic esters [11] and of *syn*-2,4-difluoroadamantane in comparison with its 1,3-difluoroadamantane isomer [127]. Some cysteine proteases have aligned backbone amide NHs in their S2 subsites and exploiting these appears to be particularly beneficial for cathepsin S inhibition [128]. The affinity reported by Tromans et al [14] for a synthetic glucose receptor is likely to reflect both frustrated hydration and secondary interactions resulting from aligned amide NH HBDs.

Frustrated hydration and potential for formation of secondary interactions are factors that are likely to be relevant to hotspot characterization [129]. A degree of molecular surface drying [130, 131] might be anticipated when hydration is frustrated although it is unclear whether this would be detectable by experiment [132]. Grand canonical Monte Carlo [133] is potentially useful for studying frustration of hydration since it is able to create and annihilate molecules in a given region, thereby allowing water molecules to be titrated in and out of the binding site.

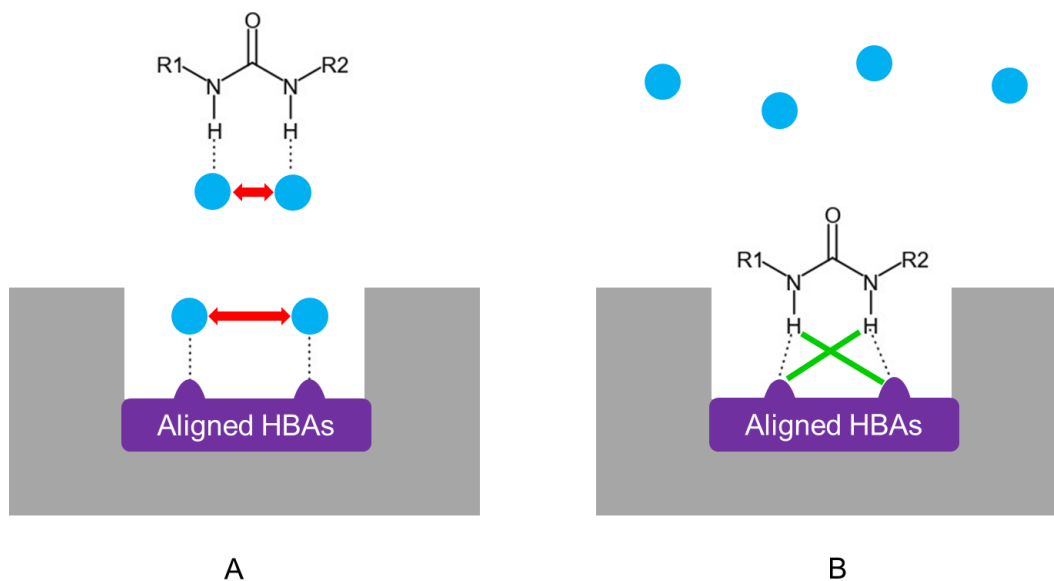


Figure 1. Unfavorable interactions between water molecules that are hydrogen bonded to target or to ligand are represented by double headed arrows (A). Secondary interactions between urea NH HBAs and aligned HBAs in binding site are represented by sticks (B).

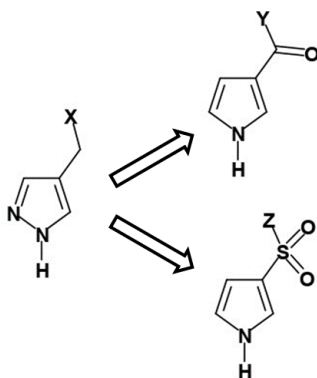
The majority of the HBAs used by designers are based either on oxygen or nitrogen. The main advantages of using a hydroxyl group are that its steric footprint is smaller than that of most nitrogen-based HBAs and it is an obvious pharmacophore element for displacing a water molecule that simultaneously donates an HB to and accepts an HB from a target. However, hydroxyl groups have undesirable characteristics from the perspective of target recognition in addition to their potential for to cause poor ADME. Donation of an HB by a ligand hydroxyl group brings the oxygen atom into proximity with the molecular surface of the target and a significant desolvation penalty for the hydroxyl oxygen can negate the benefits of HB donation if the oxygen HBA is not matched with a target HBA. As noted previously, the HBA and HBD of a hydroxyl group function in a cooperative manner and donation of an HB to the target effectively increases the hydrogen bond basicity (and desolvation penalty) of the hydroxyl oxygen atom.

Generally, designers should explore options for replacement of hydroxyl groups in the hit-to-lead phases of their projects. Although the KRAS inhibitor AZD4625 shows that the presence of a hydroxyl group does not necessarily lead to unacceptable metabolic lability [134], the phenolic hydroxyl is sterically hindered in this case. Indole and indazole have been shown to mimic a 2-chlorophenol substructure in a dopamine D₁/D₅ receptor antagonist, leading to improved pharmacokinetics, albeit at the cost of reduced potency [135]. The difluoromethyl HBA [136] lacks a co-occurring HBA and its substitution for hydroxyl would also be expected to improve metabolic stability, although HB acidity is likely to be similar to that of

dichloromethane ($\alpha_2^H = 0.13$; Table 1). There is less scope for using electron-withdrawing substituents to tune HB acidity of alkyne-based and alkene-based HBDs because of the likelihood of increased electrophilicity.

Nitrogen-based HBDs provide designers with a wider range of options than oxygen-based HBDs although this usually comes at the cost of a larger steric footprint since nitrogen is trivalent. Commonly used nitrogen-based HBDs include aromatic NH (e.g., pyrazole) and NH/NH₂ linked to carbonyl, sulfonyl or aromatic carbon in a heteroaromatic ring. One particularly notable HBD is the trifluoroethylamine of the cathepsin K inhibitor odanacatib [137] which is insufficiently basic to protonate at neutral pH on account of the strongly electron-withdrawing nature of the substituent.

In contrast to hydroxyl groups, nitrogen bonded to hydrogen cannot usually function as an HBA at physiological pH which means that any HBAs that co-occur with a nitrogen-based HBD are more distant from the donor hydrogen than is the case for an oxygen-based HBD. The co-occurring HBA issue is particularly relevant when using aromatic NH as an HBD, not least because of the potential for azoles to inhibit cytochrome P450 (CYP) metabolic enzymes. Aromatic NH is a useful molecular recognition element for designers because it allows ‘line-of-sight’ access to HBAs in target binding sites and the HBA of a 4-substituted pyrazole [138] can be moved to the linker where it may be less likely to compromise HB donation by the aromatic NH (Scheme 4). 3-Acetylpyrrole and 3-methylsulfonylpyrrole may be of interest for screening as fragments.



Scheme 4. Moving the HBA of pyrazole from ring to linker as a tactic for reducing energetically unfavorable secondary interactions with target HBAs

The ability of amines and some sp^2 nitrogen atoms (e.g., imidazole) to protonate under normal physiological conditions means that nitrogen-based HBDs can be cationic as well as neutral. Protonation of nitrogen creates very strong HBDs although basic centers not required for binding to the therapeutic target(s) should generally be avoided since these increase toxicity

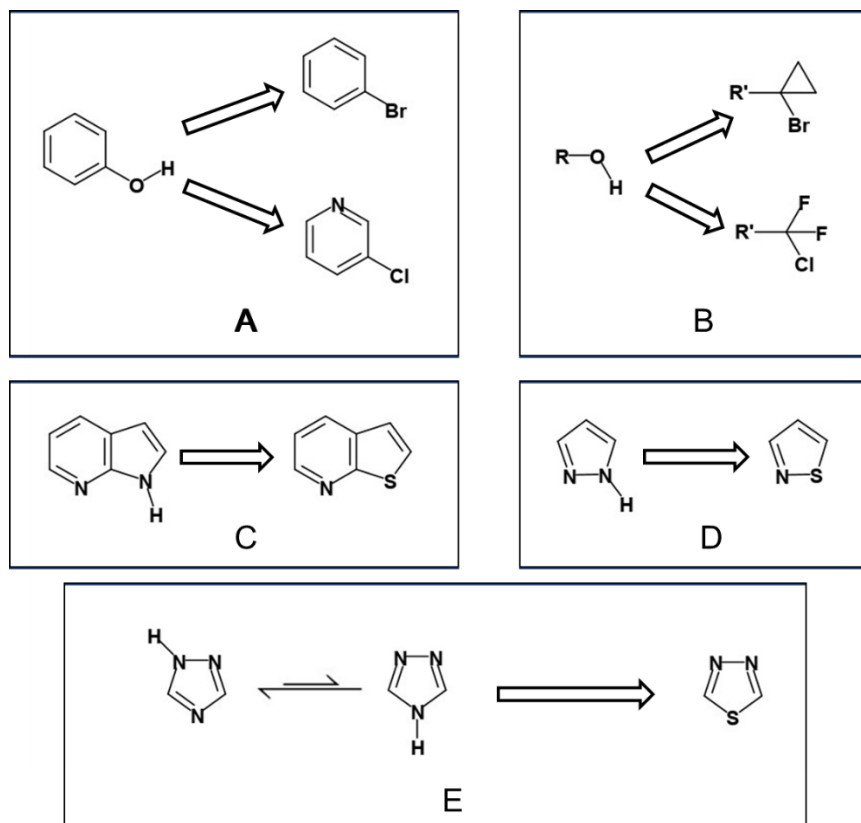
risks such as hERG blockade [139] and phospholipidosis [140]. Whether protonated or neutral, the high density of HBDs in the guanidine substructure creates opportunities for designers and its amide-like nitrogen atoms do not function as HBAs. Guanidines and amidines are often regarded as excessively basic although pK_a is actually very sensitive to substitution for these functional groups and can readily be controlled over a wide range [141, 142]. The pK_a values [141] shown in parentheses for guanidine substituted with acetyl (8.2), pyridaz-3-yl (8.3), oxazol-2-yl (5.8 for 4-methyl analog) and methylsulfonyl (1.8 for aminosulfonyl) suggest that these compounds may be of interest for screening as fragments.

Close contacts between aromatic CH and HBAs have been observed in many crystal structures [111] but the importance of these as determinants of binding affinity is rather less clear. Although HB acidity measurements do not appear to have been reported for aromatic CH HBDs, it would be reasonable to assume that the HB acidity of benzene is comparable to that of 1-heptyne ($\alpha_2^H = 0.13$; Table 1). Given that aromatic CH is a weak HBD and the large steric footprints associated with aromatic rings, it would be unusual for a designer to link a phenyl substituent to a scaffold with the primary objective of donating an HB to target. A more likely scenario would have the designer optimizing interactions made by an existing aromatic ring makes with the target. Electron-withdrawing substituents such as trifluoromethyl would be expected to increase HB acidity of aromatic CH with the collateral benefit of hardening the aromatic ring against CYP-catalyzed oxidation. Polar electron-withdrawing substituents such as aza [102] or methanesulfonyl [104] would also be expected to enhance aqueous solubility.

HBD equivalents present designers with additional options for targeting HBAs in binding sites (Scheme 5). Halogens other than fluorine can mimic a hydroxyl group by forming halogen bonds [47] with HBAs and these interactions are potentially stronger than HBs formed with carbon-based HBDs such as difluoromethyl [136]. Using a halogen as alternative to hydroxyl is a particularly appropriate tactic for targeting HBAs in narrow binding pockets because there is no co-occurring HBA and the steric footprint is smaller than for nitrogen-based HBDs. Chlorine is generally a weaker halogen bond donor than bromine although structural modifications, such as aza-substitution (Scheme 5A), that increase the extent of electron withdrawal would be expected to strengthen halogen bonding. Halogens can also be linked to non-electrophilic sp^3 carbon atoms [143, 144] (Scheme 5B) and fluoro-substitution of the carbon would be expected to strengthen the halogen bond donor.

As a chalcogen bond donor [145], sulfur can mimic [146] nitrogen-based HBDs although sulfur and NH exhibit different geometric preferences when interacting with HBAs. For example, the NH HBD in each of the kinase hinge binding substructures pyrazole (Scheme 5C)

[138] and 7-azaindole (Scheme 5D) [147] could be replaced with sulfur. Replacement of NH with sulfur can also be used to address difficulties associated with tautomerism [148] when using azoles to mimic amides. Substitution of sulfur for NH would also be expected to render a heteroaromatic ring less electron rich which may have benefits for metabolic stability.



Scheme 5. Halogen and chalcogen bond donors as HBD replacements

CONCLUSIONS

This study examines HB donor-acceptor asymmetries from the perspectives of both ADME and target recognition. Molecular structures of interest to drug designers generally have fewer HBDs than HBAs ($N_{\text{HBD}} < N_{\text{HBA}}$) and these HBDs are also likely to be less strongly hydrated than the HBAs. Published data analyses for drug-like compounds do not convincingly support the view that HBDs are more deleterious than HBAs for ADME, which may simply reflect the difficulty of varying N_{HBD} and N_{HBA} independently of each other when modelling data or the indirect nature of the analyses. Given that most of a drug's polarity is typically due to its HBAs, desolvation penalty is not generally a plausible explanation for any difficulties associated with HBDs. My view is that there is generally less scope for modulating HB acidity of HBDs in drug design than for modulating HB basicity of HBAs.

Tactics for addressing poor permeability are dictated by whether the problems are due to a surfeit of polarity or to active efflux. Efforts to address polarity-limited passive permeability

should generally be focused on HBAs rather than HBDs. Although HBDs and HBAs may both be linked to active efflux, elimination of HBDs is likely to lead to smaller increases in lipophilicity. The physicochemical rationale for elimination of HBDs as a tactic for addressing poor aqueous solubility is that N_{HBA} typically exceeds N_{HBD} for small organic molecules and the HBAs contribute more to solvation than the HBDs. This means that HBD elimination is likely to destabilize the solid state to a greater extent HBA elimination while leading to smaller increases in lipophilicity.

Designers should be alert to opportunities presented by binding site hydration that is frustrated, regardless of whether the water molecules in contact with the target are donating or accepting HBs. The range of HBDs available to designers is more restricted than for HBAs and the HBA that co-occurs with almost every HBD is a factor needs to be considered in design when presenting HBDs to targets. Nitrogen-based HBDs are generally preferred to oxygen-based HBDs although these tend to have larger steric footprints and it is typically more difficult to achieve line-of-sight access to targets. Carbon-based HBDs can be used to address ADME issues associated with heteroatom-based HBDs, especially hydroxyl groups, although the weaker HB acidity may lead to lower affinity. Alternatively, heteroatom-based HBDs could be replaced with halogen bond or chalcogen bond donors such as bromine or sulfur.

Corresponding Author

*Email, pwk.pub.2008@gmail.com

ABBREVIATIONS

ADME, absorption, distribution, metabolism and excretion; HB, hydrogen bond; HBA, hydrogen bond acceptor; HBD, hydrogen bond donor; $\log K_a$, a measure of hydrogen bond acidity; $\log P_{\text{alk}}$, base 10 logarithm of alkane/water partition coefficient, $\log P_{\text{oct}}$, base 10 logarithm of 1-octanol/water partition coefficient; MEP, molecular electrostatic potential; MMPA, matched molecular pair analysis; MSA, molecular surface area; N_{HBA} , number of hydrogen bond acceptors; N_{HBD} , number of hydrogen bond donors; $\text{p}K_a$, base 10 logarithm of acid dissociation constant; $\text{p}K_{\text{BHX}}$, hydrogen bond basicity; PSA, polar surface area; Q, polarity of a compound defined in terms of alkane/water partition coefficient and calculated molecular surface area; Ro5, rule of 5; tPSA, topological polar surface area; α_2^{H} , a measure of hydrogen bond acidity.

REFERENCES

1. Persch E, Dumele O, Diederich F (2015) Molecular Recognition in Chemical and Biological Systems. *Angewandte Chemie International Edition* 54:3290–3327. <https://doi.org/10.1002/anie.201408487>
2. Hunter CA (2004) Quantifying Intermolecular Interactions: Guidelines for the Molecular Recognition Toolbox. *Angewandte Chemie International Edition* 43:5310–5324. <https://doi.org/10.1002/anie.200301739>
3. Smith DK (2005) A Supramolecular Approach to Medicinal Chemistry: Medicine Beyond the Molecule. *J Chem Educ* 82:393. <https://doi.org/10.1021/ed082p393>
4. Bissantz C, Kuhn B, Stahl M (2010) A Medicinal Chemist's Guide to Molecular Interactions. *J Med Chem* 53:5061–5084. <https://doi.org/10.1021/jm100112j>
5. Yang L, Adam C, Nichol GS, Cockroft SL (2013) How much do van der Waals dispersion forces contribute to molecular recognition in solution? *Nature Chem* 5:1006–1010. <https://doi.org/10.1038/nchem.1779>
6. Jeffrey GA (1997) An introduction to hydrogen bonding. Oxford University Press, New York
7. Gilli G, Gilli P (2009) The nature of the hydrogen bond: outline of a comprehensive hydrogen bond theory. Oxford University Press, Oxford ; New York
8. Taylor R, Kennard O (1984) Hydrogen-bond geometry in organic crystals. *Acc Chem Res* 17:320–326. <https://doi.org/10.1021/ar00105a004>
9. Abraham MH, Duce PP, Prior DV, et al (1989) Hydrogen bonding. Part 9. Solute proton donor and proton acceptor scales for use in drug design. *J Chem Soc, Perkin Trans 2* 1355–1375. <https://doi.org/10.1039/P29890001355>
10. Abraham MH (1993) Scales of solute hydrogen-bonding: their construction and application to physicochemical and biochemical processes. *Chem Soc Rev* 22:73–83. <https://doi.org/10.1039/CS9932200073>
11. Laurence C, Berthelot M (2000) Observations on the strength of hydrogen bonding. *Perspectives in Drug Discovery and Design* 18:39–60. <https://doi.org/10.1023/A:1008743229409>
12. Laurence C, Brameld KA, Graton J, et al (2009) The pK_{BHX} Database: Toward a Better Understanding of Hydrogen-Bond Basicity for Medicinal Chemists. *J Med Chem* 52:4073–4086. <https://doi.org/10.1021/jm801331y>
13. Wells TNC, Fersht AR (1985) Hydrogen bonding in enzymatic catalysis analysed by protein engineering. *Nature* 316:656–657. <https://doi.org/10.1038/316656a0>
14. Tromans RA, Carter TS, Chabanne L, et al (2019) A biomimetic receptor for glucose. *Nature Chem* 11:52–56. <https://doi.org/10.1038/s41557-018-0155-z>
15. Etter MC (1990) Encoding and decoding hydrogen-bond patterns of organic compounds. *Acc Chem Res* 23:120–126. <https://doi.org/10.1021/ar00172a005>
16. Desiraju GR (2007) Crystal Engineering: A Holistic View. *Angew Chem Int Ed* 46:8342–8356. <https://doi.org/10.1002/anie.200700534>
17. Southall NT, Dill KA, Haymet ADJ (2002) A View of the Hydrophobic Effect. *J Phys Chem B* 106:521–533. <https://doi.org/10.1021/jp015514e>
18. Costales MG, Childs-Disney JL, Haniff HS, Disney MD (2020) How We Think about Targeting RNA with Small Molecules. *J Med Chem* 63:8880–8900. <https://doi.org/10.1021/acs.jmedchem.9b01927>
19. Kenny PW (2019) The nature of ligand efficiency. *Journal of Cheminformatics* 11:8. <https://doi.org/10.1186/s13321-019-0330-2>
20. Fersht AR, Shi J-P, Knill-Jones J, et al (1985) Hydrogen bonding and biological specificity analysed by protein engineering. *Nature* 314:235–238. <https://doi.org/10.1038/314235a0>

21. Shen Y, Gilson MK, Tidor B (2012) Charge Optimization Theory for Induced-Fit Ligands. *J Chem Theory Comput* 8:4580–4592. <https://doi.org/10.1021/ct200931c>
22. Kenny PW, Montanari CA, Prokopczyk IM, et al (2016) Hydrogen Bond Basicity Prediction for Medicinal Chemistry Design. *J Med Chem* 59:4278–4288. <https://doi.org/10.1021/acs.jmedchem.5b01946>
23. Mateus A, Matsson P, Artursson P (2013) Rapid Measurement of Intracellular Unbound Drug Concentrations. *Mol Pharmaceutics* 10:2467–2478. <https://doi.org/10.1021/mp4000822>
24. Smith DA, Rowland M (2019) Intracellular and Intraorgan Concentrations of Small Molecule Drugs: Theory, Uncertainties in Infectious Diseases and Oncology, and Promise. *Drug Metab Dispos* 47:665–672. <https://doi.org/10.1124/dmd.118.085951>
25. Owen DR, Allerton CMN, Anderson AS, et al (2021) An oral SARS-CoV-2 M^{pro} inhibitor clinical candidate for the treatment of COVID-19. *Science* 374:1586–1593. <https://doi.org/10.1126/science.abl4784>
26. Baell J, Congreve M, Leeson P, Abad-Zapatero C (2013) Ask the Experts: Past, present and future of the rule of five. *Future Medicinal Chemistry* 5:745–752. <https://doi.org/10.4155/fmc.13.61>
27. Rowland A, Miners JO, Mackenzie PI (2013) The UDP-glucuronosyltransferases: Their role in drug metabolism and detoxification. *The International Journal of Biochemistry & Cell Biology* 45:1121–1132. <https://doi.org/10.1016/j.biocel.2013.02.019>
28. Lovering F (2013) Escape from Flatland 2: complexity and promiscuity. *Med Chem Commun* 4:515–519. <https://doi.org/10.1039/C2MD20347B>
29. Mobley DL, Barber AE, Fennell CJ, Dill KA (2008) Charge Asymmetries in Hydration of Polar Solutes. *J Phys Chem B* 112:2405–2414. <https://doi.org/10.1021/jp709958f>
30. Taft RW, Gurka D, Joris L, et al (1969) Studies of hydrogen-bonded complex formation with p-fluorophenol. V. Linear free energy relationships with OH reference acids. *J Am Chem Soc* 91:4801–4808. <https://doi.org/10.1021/ja01045a038>
31. Frange B, Abboud JLM, Benamou C, Bellon L (1982) A quantitative study of structural effects on the self-association of alcohols. *J Org Chem* 47:4553–4557. <https://doi.org/10.1021/jo00144a029>
32. Abraham MH, Duce PP, Morris JJ, Taylor PJ (1987) Hydrogen bonding. Part 2.—Equilibrium constants and enthalpies of complexation for 72 monomeric hydrogen-bond acids with N-methylpyrrolidinone in 1,1,1-trichloroethane. *J Chem Soc, Faraday Trans 1* 83:2867. <https://doi.org/10.1039/f19878302867>
33. Laurence C, Queignec R (1992) A thermodynamic hydrogen-bond acidity scale for monosubstituted acetylenes. *J Chem Soc, Perkin Trans 2* 1915–1917. <https://doi.org/10.1039/p29920001915>
34. Morris JJ, Hughes LR, Glen AT, Taylor PJ (1991) Non-steroidal antiandrogens. Design of novel compounds based on an infrared study of the dominant conformation and hydrogen-bonding properties of a series of anilide antiandrogens. *J Med Chem* 34:447–455. <https://doi.org/10.1021/jm00105a067>
35. Abraham MH, Abraham RJ, Byrne J, Griffiths L (2006) NMR Method for the Determination of Solute Hydrogen Bond Acidity. *J Org Chem* 71:3389–3394. <https://doi.org/10.1021/jo052631n>
36. Abraham MR, Duce PP, Grellier PL, et al (1988) Hydrogen-bonding. Part 5. A thermodynamically-based scale of solute hydrogen-bond acidity. *Tetrahedron Letters* 29:1587–1590. [https://doi.org/10.1016/S0040-4039\(00\)80360-3](https://doi.org/10.1016/S0040-4039(00)80360-3)
37. Abraham MH, Grellier PL, Prior DV, et al (1989) Hydrogen bonding. Part 7. A scale of solute hydrogen-bond acidity based on log K values for complexation in tetrachloromethane. *J Chem Soc, Perkin Trans 2* 699–711. <https://doi.org/10.1039/p29890000699>
38. Abraham MH, Grellier PL, Prior DV, et al (1990) Hydrogen-bonding. Part 11. A quantitative evaluation of the hydrogen-bond acidity of imides as solutes. *J Org Chem* 55:2227–2229. <https://doi.org/10.1021/jo00294a045>

39. Abraham MH, Berthelot M, Laurence C, Taylor PJ (1998) Analysis of hydrogen-bond complexation constants in 1,1,1-trichloroethane: the $\alpha_2^H\beta_2^H$ relationship. *J Chem Soc, Perkin Trans 2* 187–192. <https://doi.org/10.1039/a702326j>
40. Graton J, Besseau F, Brossard A-M, et al (2013) Hydrogen-Bond Acidity of OH Groups in Various Molecular Environments (Phenols, Alcohols, Steroid Derivatives, and Amino Acids Structures): Experimental Measurements and Density Functional Theory Calculations. *J Phys Chem A* 117:13184–13193. <https://doi.org/10.1021/jp410027h>
41. Abraham MH, Gil-Lostes J, Enrique Cometto-Muñiz J, et al (2009) The hydrogen bond acidity and other descriptors for oximes. *New J Chem* 33:76–81. <https://doi.org/10.1039/B811688A>
42. Abraham MH, Grellier PL, Prior DV, et al (1988) A general treatment of hydrogen bond complexation constants in tetrachloromethane. *J Am Chem Soc* 110:8534–8536. <https://doi.org/10.1021/ja00233a034>
43. Jorgensen WL, Pranata J (1990) Importance of secondary interactions in triply hydrogen bonded complexes: guanine-cytosine vs uracil-2,6-diaminopyridine. *J Am Chem Soc* 112:2008–2010. <https://doi.org/10.1021/ja00161a061>
44. Hagelin H, Murray JS, Politzer P, et al (1995) Family-independent relationships between computed molecular surface quantities and solute hydrogen bond acidity/basicity and solute-induced methanol O–H infrared frequency shifts. *Can J Chem* 73:483–488. <https://doi.org/10.1139/v95-063>
45. Kenny PW (2009) Hydrogen Bonding, Electrostatic Potential, and Molecular Design. *J Chem Inf Model* 49:1234–1244. <https://doi.org/10.1021/ci9000234>
46. Laurence C, Graton J, Berthelot M, El Ghomari MJ (2011) The Diiodine Basicity Scale: Toward a General Halogen-Bond Basicity Scale. *Chem Eur J* 17:10431–10444. <https://doi.org/10.1002/chem.201101071>
47. Gilday LC, Robinson SW, Barendt TA, et al (2015) Halogen Bonding in Supramolecular Chemistry. *Chem Rev* 115:7118–7195. <https://doi.org/10.1021/cr500674c>
48. Borges NM, Kenny PW, Montanari CA, et al (2017) The influence of hydrogen bonding on partition coefficients. *J Comput Aided Mol Des* 31:163–181. <https://doi.org/10.1007/s10822-016-0002-5>
49. Collander R, Lindholm M, Haug CM, et al (1951) The Partition of Organic Compounds Between Higher Alcohols and Water. *Acta Chem Scand* 5:774–780. <https://doi.org/10.3891/acta.chem.scand.05-0774>
50. Hansch C, Muir RM, Fujita T, et al (1963) The Correlation of Biological Activity of Plant Growth Regulators and Chloromycetin Derivatives with Hammett Constants and Partition Coefficients. *J Am Chem Soc* 85:2817–2824. <https://doi.org/10.1021/ja00901a033>
51. Leo A, Hansch C, Elkins D (1971) Partition coefficients and their uses. *Chem Rev* 71:525–616. <https://doi.org/10.1021/cr60274a001>
52. Abraham MH, Chadha HS, Whiting GS, Mitchell RC (1994) Hydrogen Bonding. 32. An Analysis of Water-Octanol and Water-Alkane Partitioning and the $\Delta\log P$ Parameter of Seiler. *J PharmSci* 83:1085–1100. <https://doi.org/10.1002/jps.2600830806>
53. Kenny PW, Montanari CA (2013) Inflation of correlation in the pursuit of drug-likeness. *J Comput Aided Mol Des* 27:1–13. <https://doi.org/10.1007/s10822-012-9631-5>
54. Golumbic C, Orchin M, Weller S (1949) Partition Studies on Phenols. I. Relation between Partition Coefficient and Ionization Constant. *J Am Chem Soc* 71:2624–2627. <https://doi.org/10.1021/ja01176a006>
55. Seiler P (1974) Interconversion of lipophilicities from hydrocarbon-water systems into octanol-water system. *European Journal of Medicinal Chemistry* 9:473–479
56. Finkelstein A (1976) Water and nonelectrolyte permeability of lipid bilayer membranes. *J Gen Physiol* 68:127–135. <https://doi.org/10.1085/jgp.68.2.127>
57. Riebesehl W, Tomlinson E (1984) Enthalpies of solute transfer between alkanes and water determined directly by flow microcalorimetry. *J Phys Chem* 88:4770–4775. <https://doi.org/10.1021/j150664a064>

58. Radzicka A, Wolfenden R (1988) Comparing the polarities of the amino acids: side-chain distribution coefficients between the vapor phase, cyclohexane, 1-octanol, and neutral aqueous solution. *Biochemistry* 27:1664–1670. <https://doi.org/10.1021/bi00405a042>
59. Abraham MH, Whiting GS, Fuchs R, Chambers EJ (1990) Thermodynamics of solute transfer from water to hexadecane. *J Chem Soc, Perkin Trans 2* 291–300. <https://doi.org/10.1039/P29900000291>
60. Leahy DE, Morris JJ, Taylor PJ, Wait AR (1992) Model solvent systems for QSAR. Part 2. Fragment values ('f-values') for the 'critical quartet.' *J Chem Soc, Perkin Trans 2* 723–731. <https://doi.org/10.1039/P29920000723>
61. Shih P, Pedersen LG, Gibbs PR, Wolfenden R (1998) Hydrophobicities of the nucleic acid bases: distribution coefficients from water to cyclohexane. *Journal of Molecular Biology* 280:421–430. <https://doi.org/10.1006/jmbi.1998.1880>
62. Dearden JC, Bresnen GM (2005) Thermodynamics of Water-octanol and Water-cyclohexane Partitioning of some Aromatic Compounds. *International Journal of Molecular Sciences* 6:119–129. <https://doi.org/10.3390/i6010119>
63. Toulmin A, Wood JM, Kenny PW (2008) Toward Prediction of Alkane/Water Partition Coefficients. *J Med Chem* 51:3720–3730. <https://doi.org/10.1021/jm701549s>
64. Bard B, Carrupt P-A, Martel S (2012) Determination of alkane/water partition coefficients of polar compounds using hydrophilic interaction chromatography. *Journal of Chromatography A* 1260:164–168. <https://doi.org/10.1016/j.chroma.2012.08.094>
65. Jensen DA, Gary RK (2015) Estimation of alkane–water logP for neutral, acidic, and basic compounds using an alkylated polystyrene-divinylbenzene high-performance liquid chromatography column. *Journal of Chromatography A* 1417:21–29. <https://doi.org/10.1016/j.chroma.2015.09.020>
66. Rustenburg AS, Dancer J, Lin B, et al (2016) Measuring experimental cyclohexane-water distribution coefficients for the SAMPL5 challenge. *J Comput Aided Mol Des* 30:945–958. <https://doi.org/10.1007/s10822-016-9971-7>
67. Kenny PW, Montanari CA, Prokopczyk IM (2013) ClogPalk: a method for predicting alkane/water partition coefficient. *J Comput Aided Mol Des* 27:389–402. <https://doi.org/10.1007/s10822-013-9655-5>
68. Avdeef A (1992) pH-Metric log P. Part 1. Difference Plots for Determining Ion-Pair Octanol-Water Partition Coefficients of Multiprotic Substances. *Quant Struct-Act Relat* 11:510–517. <https://doi.org/10.1002/qsar.2660110408>
69. Scherrer RA, Donovan SF (2009) Automated Potentiometric Titrations in KCl/Water-Saturated Octanol: Method for Quantifying Factors Influencing Ion-Pair Partitioning. *Anal Chem* 81:2768–2778. <https://doi.org/10.1021/ac802729k>
70. Cabani S, Gianni P, Mollica V, Lepori L (1981) Group contributions to the thermodynamic properties of non-ionic organic solutes in dilute aqueous solution. *J Solution Chem* 10:563–595. <https://doi.org/10.1007/BF00646936>
71. El Tayar N, Testa B, Carrupt PA (1992) Polar intermolecular interactions encoded in partition coefficients: an indirect estimation of hydrogen-bond parameters of polyfunctional solutes. *J Phys Chem* 96:1455–1459. <https://doi.org/10.1021/j100182a078>
72. Kenny PW (2020) Hydrogen bond basicity data. Figshare <https://doi.org/10.6084/m9.figshare.12084183.v1>
73. Berthelot M, Laurence C, Foucher D, Taft RW (1996) Partition coefficients and intramolecular hydrogen bonding. 1. The hydrogen-bond basicity of intramolecular hydrogen-bonded heteroatoms. *J Phys Org Chem* 9:255–261. [https://doi.org/10.1002/\(SICI\)1099-1395\(199605\)9:5<255::AID-POC779>3.0.CO;2-G](https://doi.org/10.1002/(SICI)1099-1395(199605)9:5<255::AID-POC779>3.0.CO;2-G)

74. Augustijns PF, Brown SC, Willard DH, et al (2000) Hydration Changes Implicated in the Remarkable Temperature-Dependent Membrane Permeation of Cyclosporin A. *Biochemistry* 39:7621–7630. <https://doi.org/10.1021/bi9929709>
75. Shalaeva M, Caron G, Abramov YA, et al (2013) Integrating Intramolecular Hydrogen Bonding (IMHB) Considerations in Drug Discovery Using $\Delta\log P$ As a Tool. *J Med Chem* 56:4870–4879. <https://doi.org/10.1021/jm301850m>
76. McDonald IK, Thornton JM (1994) Satisfying Hydrogen Bonding Potential in Proteins. *Journal of Molecular Biology* 238:777–793. <https://doi.org/10.1006/jmbi.1994.1334>
77. Lipinski CA, Lombardo F, Dominy BW, Feeney PJ (1997) Experimental and computational approaches to estimate solubility and permeability in drug discovery and development settings. *Advanced Drug Delivery Reviews* 23:3–25. [https://doi.org/10.1016/S0169-409X\(96\)00423-1](https://doi.org/10.1016/S0169-409X(96)00423-1)
78. Stepan AF, Walker DP, Bauman J, et al (2011) Structural Alert/Reactive Metabolite Concept as Applied in Medicinal Chemistry to Mitigate the Risk of Idiosyncratic Drug Toxicity: A Perspective Based on the Critical Examination of Trends in the Top 200 Drugs Marketed in the United States. *Chem Res Toxicol* 24:1345–1410. <https://doi.org/10.1021/tx200168d>
79. Leeson PD, Davis AM (2004) Time-Related Differences in the Physical Property Profiles of Oral Drugs. *J Med Chem* 47:6338–6348. <https://doi.org/10.1021/jm049717d>
80. Shultz MD (2019) Two Decades under the Influence of the Rule of Five and the Changing Properties of Approved Oral Drugs: Miniperspective. *J Med Chem* 62:1701–1714. <https://doi.org/10.1021/acs.jmedchem.8b00686>
81. Pinkerton AA, Schwarzenbach D (1978) Structural studies on biguanide and related species. Correlation of protonation energy with molecular structure. *J Chem Soc, Dalton Trans* 989. <https://doi.org/10.1039/dt9780000989>
82. Veber DF, Johnson SR, Cheng H-Y, et al (2002) Molecular Properties That Influence the Oral Bioavailability of Drug Candidates. *J Med Chem* 45:2615–2623. <https://doi.org/10.1021/jm020017n>
83. Vieth M, Siegel MG, Higgs RE, et al (2004) Characteristic Physical Properties and Structural Fragments of Marketed Oral Drugs. *J Med Chem* 47:224–232. <https://doi.org/10.1021/jm030267j>
84. Oprea TI (2000) Property distribution of drug-related chemical databases. *Journal of Computer-Aided Molecular Design* 14:251–264. <https://doi.org/10.1023/A:1008130001697>
85. Raschka S, Wolf AJ, Bemister-Buffington J, Kuhn LA (2018) Protein–ligand interfaces are polarized: discovery of a strong trend for intermolecular hydrogen bonds to favor donors on the protein side with implications for predicting and designing ligand complexes. *J Comput Aided Mol Des* 32:511–528. <https://doi.org/10.1007/s10822-018-0105-2>
86. Xu Y, Shrestha N, Pr at V, Belouqui A (2021) An overview of in vitro, ex vivo and in vivo models for studying the transport of drugs across intestinal barriers. *Advanced Drug Delivery Reviews* 175:113795. <https://doi.org/10.1016/j.addr.2021.05.005>
87. Berben P, Bauer-Brandl A, Brandl M, et al (2018) Drug permeability profiling using cell-free permeation tools: Overview and applications. *European Journal of Pharmaceutical Sciences* 119:219–233. <https://doi.org/10.1016/j.ejps.2018.04.016>
88. Sharifian Gh. M (2021) Recent Experimental Developments in Studying Passive Membrane Transport of Drug Molecules. *Mol Pharmaceutics* 18:2122–2141. <https://doi.org/10.1021/acs.molpharmaceut.1c00009>
89. Volpe DA (2011) Drug-permeability and transporter assays in Caco-2 and MDCK cell lines. *Future Medicinal Chemistry* 3:2063–2077. <https://doi.org/10.4155/fmc.11.149>
90. Klein VG, Bond AG, Craigon C, et al (2021) Amide-to-Ester Substitution as a Strategy for Optimizing PROTAC Permeability and Cellular Activity. *J Med Chem* 64:18082–18101. <https://doi.org/10.1021/acs.jmedchem.1c01496>

91. Rankovic Z (2015) CNS Drug Design: Balancing Physicochemical Properties for Optimal Brain Exposure. *J Med Chem* 58:2584–2608. <https://doi.org/10.1021/jm501535r>
92. Di L, Kerns EH, Bezar IF, et al (2009) Comparison of blood–brain barrier permeability assays: in situ brain perfusion, MDR1-MDCKII and PAMPA-BBB. *Journal of Pharmaceutical Sciences* 98:1980–1991. <https://doi.org/10.1002/jps.21580>
93. Bicker J, Alves G, Fortuna A, Falcão A (2014) Blood–brain barrier models and their relevance for a successful development of CNS drug delivery systems: A review. *European Journal of Pharmaceutics and Biopharmaceutics* 87:409–432. <https://doi.org/10.1016/j.ejpb.2014.03.012>
94. Hitchcock SA, Pennington LD (2006) Structure–Brain Exposure Relationships. *J Med Chem* 49:7559–7583. <https://doi.org/10.1021/jm060642i>
95. Wager TT, Hou X, Verhoest PR, Villalobos A (2016) Central Nervous System Multiparameter Optimization Desirability: Application in Drug Discovery. *ACS Chem Neurosci* 7:767–775. <https://doi.org/10.1021/acchemneuro.6b00029>
96. Young RC, Mitchell RC, Brown TH, et al (1988) Development of a new physicochemical model for brain penetration and its application to the design of centrally acting H₂ receptor histamine antagonists. *J Med Chem* 31:656–671. <https://doi.org/10.1021/jm00398a028>
97. Hitchcock SA (2012) Structural Modifications that Alter the P-Glycoprotein Efflux Properties of Compounds. *J Med Chem* 55:4877–4895. <https://doi.org/10.1021/jm201136z>
98. Giblin GMP, Billinton A, Briggs M, et al (2009) Discovery of 1-[4-(3-Chlorophenylamino)-1-methyl-1*H*-pyrrolo[3,2-*c*]pyridin-7-yl]-1-morpholin-4-ylmethanone (GSK554418A), a Brain Penetrant 5-Azaindole CB₂ Agonist for the Treatment of Chronic Pain. *J Med Chem* 52:5785–5788. <https://doi.org/10.1021/jm9009857>
99. Weiss MM, Williamson T, Babu-Khan S, et al (2012) Design and Preparation of a Potent Series of Hydroxyethylamine Containing β -Secretase Inhibitors That Demonstrate Robust Reduction of Central β -Amyloid. *J Med Chem* 55:9009–9024. <https://doi.org/10.1021/jm300119p>
100. Augustijns P, Wuyts B, Hens B, et al (2014) A review of drug solubility in human intestinal fluids: Implications for the prediction of oral absorption. *European Journal of Pharmaceutical Sciences* 57:322–332. <https://doi.org/10.1016/j.ejps.2013.08.027>
101. Hann MM, Leach AR, Harper G (2001) Molecular Complexity and Its Impact on the Probability of Finding Leads for Drug Discovery. *J Chem Inf Comput Sci* 41:856–864. <https://doi.org/10.1021/ci000403i>
102. Birch AM, Kenny PW, Simpson I, Whittamore PRO (2009) Matched molecular pair analysis of activity and properties of glycogen phosphorylase inhibitors. *Bioorganic & Medicinal Chemistry Letters* 19:850–853. <https://doi.org/10.1016/j.bmcl.2008.12.003>
103. Yamasaki R, Tanatani A, Azumaya I, et al (2003) Amide Conformational Switching Induced by Protonation of Aromatic Substituent. *Org Lett* 5:1265–1267. <https://doi.org/10.1021/ol034344g>
104. Leach AG, Jones HD, Cosgrove DA, et al (2006) Matched Molecular Pairs as a Guide in the Optimization of Pharmaceutical Properties; a Study of Aqueous Solubility, Plasma Protein Binding and Oral Exposure. *J Med Chem* 49:6672–6682. <https://doi.org/10.1021/jm0605233>
105. Ritchie TJ, Macdonald SJF (2014) Physicochemical Descriptors of Aromatic Character and Their Use in Drug Discovery: Miniperspective. *J Med Chem* 57:7206–7215. <https://doi.org/10.1021/jm500515d>
106. Lovering F, Bikker J, Humblet C (2009) Escape from Flatland: Increasing Saturation as an Approach to Improving Clinical Success. *J Med Chem* 52:6752–6756. <https://doi.org/10.1021/jm901241e>
107. Ishikawa M, Hashimoto Y (2011) Improvement in Aqueous Solubility in Small Molecule Drug Discovery Programs by Disruption of Molecular Planarity and Symmetry. *J Med Chem* 54:1539–1554. <https://doi.org/10.1021/jm101356p>

108. Auberson YP, Brocklehurst C, Furegati M, et al (2017) Improving Nonspecific Binding and Solubility: Bicycloalkyl Groups and Cubanes as *para*-Phenyl Bioisosteres. *ChemMedChem* 12:590–598. <https://doi.org/10.1002/cmdc.201700082>
109. Hunter CA, Lawson KR, Perkins J, Urch CJ (2001) Aromatic interactions. *J Chem Soc, Perkin Trans 2* 651–669. <https://doi.org/10.1039/b008495f>
110. Meyer EA, Castellano RK, Diederich F (2003) Interactions with Aromatic Rings in Chemical and Biological Recognition. *Angew Chem Int Ed* 42:1210–1250. <https://doi.org/10.1002/anie.200390319>
111. Desiraju GR (1996) The C–H···O Hydrogen Bond: Structural Implications and Supramolecular Design. *Acc Chem Res* 29:441–449. <https://doi.org/10.1021/ar950135n>
112. Lee L-P, Tidor B (1997) Optimization of electrostatic binding free energy. *The Journal of Chemical Physics* 106:8681–8690. <https://doi.org/10.1063/1.473929>
113. Samways ML, Taylor RD, Bruce Macdonald HE, Essex JW (2021) Water molecules at protein–drug interfaces: computational prediction and analysis methods. *Chem Soc Rev* 50:9104–9120. <https://doi.org/10.1039/D0CS00151A>
114. Barillari C, Taylor J, Viner R, Essex JW (2007) Classification of Water Molecules in Protein Binding Sites. *J Am Chem Soc* 129:2577–2587. <https://doi.org/10.1021/ja066980q>
115. Olsson TSG, Williams MA, Pitt WR, Ladbury JE (2008) The Thermodynamics of Protein–Ligand Interaction and Solvation: Insights for Ligand Design. *Journal of Molecular Biology* 384:1002–1017. <https://doi.org/10.1016/j.jmb.2008.09.073>
116. Biedermannová L, Schneider B (2016) Hydration of proteins and nucleic acids: Advances in experiment and theory. A review. *Biochimica et Biophysica Acta (BBA) - General Subjects* 1860:1821–1835. <https://doi.org/10.1016/j.bbagen.2016.05.036>
117. Spyrakis F, Ahmed MH, Bayden AS, et al (2017) The Roles of Water in the Protein Matrix: A Largely Untapped Resource for Drug Discovery. *J Med Chem* 60:6781–6827. <https://doi.org/10.1021/acs.jmedchem.7b00057>
118. Franck JM, Han S (2019) Overhauser Dynamic Nuclear Polarization for the Study of Hydration Dynamics, Explained. *Methods in Enzymology* 615:131–175. <https://doi.org/10.1016/bs.mie.2018.09.024>
119. Maurer M, Oostenbrink C (2019) Water in protein hydration and ligand recognition. *J Mol Recognit* 32:. <https://doi.org/10.1002/jmr.2810>
120. Nguyen C, Yamazaki T, Kovalenko A, et al (2019) A molecular reconstruction approach to site-based 3D-RISM and comparison to GIST hydration thermodynamic maps in an enzyme active site. *PLoS ONE* 14:e0219473. <https://doi.org/10.1371/journal.pone.0219473>
121. Dunitz JD (1994) The Entropic Cost of Bound Water in Crystals and Biomolecules. *Science* 264:670–670. <https://doi.org/10.1126/science.264.5159.670>
122. Russo D, Murarka RK, Copley JRD, Head-Gordon T (2005) Molecular View of Water Dynamics near Model Peptides. *J Phys Chem B* 109:12966–12975. <https://doi.org/10.1021/jp051137k>
123. Johnson ME, Malardier-Jugroot C, Murarka RK, Head-Gordon T (2009) Hydration Water Dynamics Near Biological Interfaces. *J Phys Chem B* 113:4082–4092. <https://doi.org/10.1021/jp806183v>
124. Jencks WP (1981) On the attribution and additivity of binding energies. *PNAS* 78:4046–4050. <https://doi.org/10.1073/pnas.78.7.4046>
125. McConnell DB (2021) Biotin’s Lessons in Drug Design. *J Med Chem* 64:16319–16327. <https://doi.org/10.1021/acs.jmedchem.1c00975>
126. Le Trong I, Wang Z, Hyre DE, et al (2011) Streptavidin and its biotin complex at atomic resolution. *Acta Crystallogr D Biol Crystallogr* 67:813–821. <https://doi.org/10.1107/S0907444911027806>

127. Adcock W, Graton J, Laurence C, et al (2005) Three-centre hydrogen bonding in the complexes of *syn*-2,4-difluoroadamantane with 4-fluorophenol and hydrogen fluoride. *J Phys Org Chem* 18:227–234. <https://doi.org/10.1002/poc.813>
128. Bethel PA, Gerhardt S, Jones EV, et al (2009) Design of selective Cathepsin inhibitors. *Bioorganic & Medicinal Chemistry Letters* 19:4622–4625. <https://doi.org/10.1016/j.bmcl.2009.06.090>
129. Radoux CJ, Olsson TSG, Pitt WR, et al (2016) Identifying Interactions that Determine Fragment Binding at Protein Hotspots. *J Med Chem* 59:4314–4325. <https://doi.org/10.1021/acs.jmedchem.5b01980>
130. Rasaiah JC, Garde S, Hummer G (2008) Water in Nonpolar Confinement: From Nanotubes to Proteins and Beyond. *Annu Rev Phys Chem* 59:713–740. <https://doi.org/10.1146/annurev.physchem.59.032607.093815>
131. Beuming T, Che Y, Abel R, et al (2012) Thermodynamic analysis of water molecules at the surface of proteins and applications to binding site prediction and characterization. *Proteins* 80:871–883. <https://doi.org/10.1002/prot.23244>
132. Krimmer SG, Cramer J, Schiebel J, et al (2017) How Nothing Boosts Affinity: Hydrophobic Ligand Binding to the Virtually Vacated S₁' Pocket of Thermolysin. *J Am Chem Soc* 139:10419–10431. <https://doi.org/10.1021/jacs.7b05028>
133. Ross GA, Bruce Macdonald HE, Cave-Ayland C, et al (2017) Replica-Exchange and Standard State Binding Free Energies with Grand Canonical Monte Carlo. *J Chem Theory Comput* 13:6373–6381. <https://doi.org/10.1021/acs.jctc.7b00738>
134. Kettle JG, Bagal SK, Bickerton S, et al (2022) Discovery of AZD4625, a Covalent Allosteric Inhibitor of the Mutant GTPase KRAS^{G12C}. *J Med Chem* [acs.jmedchem.2c00369](https://doi.org/10.1021/acs.jmedchem.2c00369). <https://doi.org/10.1021/acs.jmedchem.2c00369>
135. Wu W-L, Burnett DA, Spring R, et al (2005) Dopamine D₁/D₅ Receptor Antagonists with Improved Pharmacokinetics: Design, Synthesis, and Biological Evaluation of Phenol Bioisosteric Analogues of Benzazepine D₁/D₅ Antagonists. *J Med Chem* 48:680–693. <https://doi.org/10.1021/jm030614p>
136. Zafrani Y, Yeffet D, Sod-Moriah G, et al (2017) Difluoromethyl Bioisostere: Examining the “Lipophilic Hydrogen Bond Donor” Concept. *J Med Chem* 60:797–804. <https://doi.org/10.1021/acs.jmedchem.6b01691>
137. Gauthier JY, Chauret N, Cromlish W, et al (2008) The discovery of odanacatib (MK-0822), a selective inhibitor of cathepsin K. *Bioorganic & Medicinal Chemistry Letters* 18:923–928. <https://doi.org/10.1016/j.bmcl.2007.12.047>
138. Saxty G, Woodhead SJ, Berdini V, et al (2007) Identification of Inhibitors of Protein Kinase B Using Fragment-Based Lead Discovery. *J Med Chem* 50:2293–2296. <https://doi.org/10.1021/jm070091b>
139. Jamieson C, Moir EM, Rankovic Z, Wishart G (2006) Medicinal Chemistry of hERG Optimizations: Highlights and Hang-Ups. *J Med Chem* 49:5029–5046. <https://doi.org/10.1021/jm060379l>
140. Tummino TA, Rezelj VV, Fischer B, et al (2021) Drug-induced phospholipidosis confounds drug repurposing for SARS-CoV-2. *Science* 373:541–547. <https://doi.org/10.1126/science.abi4708>
141. Taylor PJ, Wait AR (1986) σ_1 Values for heterocycles. *J Chem Soc, Perkin Trans 2* 1765–1770. <https://doi.org/10.1039/P29860001765>
142. Eldred CD, Evans B, Hindley S, et al (1994) Orally Active Non-Peptide Fibrinogen Receptor (GpIIb/IIIa) Antagonists: Identification of 4-[4-[4-(Aminoimino methyl)phenyl]-1-piperazinyl]-1-piperidineacetic Acid as a Long-Acting, Broad-Spectrum Antithrombotic Agent. *J Med Chem* 37:3882–3885. <https://doi.org/10.1021/jm00049a006>
143. Schoenfeld RC, Bourdet DL, Brameld KA, et al (2013) Discovery of a Novel Series of Potent Non-Nucleoside Inhibitors of Hepatitis C Virus NS5B. *J Med Chem* 56:8163–8182. <https://doi.org/10.1021/jm401266k>

144. Schoepfer J, Jahnke W, Berellini G, et al (2018) Discovery of Asciminib (ABL001), an Allosteric Inhibitor of the Tyrosine Kinase Activity of BCR-ABL1. *J Med Chem* 61:8120–8135. <https://doi.org/10.1021/acs.jmedchem.8b01040>
145. Pascoe DJ, Ling KB, Cockroft SL (2017) The Origin of Chalcogen-Bonding Interactions. *J Am Chem Soc* 139:15160–15167. <https://doi.org/10.1021/jacs.7b08511>
146. Beno BR, Yeung K-S, Bartberger MD, et al (2015) A Survey of the Role of Noncovalent Sulfur Interactions in Drug Design. *J Med Chem* 58:4383–4438. <https://doi.org/10.1021/jm501853m>
147. Tsai J, Lee JT, Wang W, et al (2008) Discovery of a selective inhibitor of oncogenic B-Raf kinase with potent antimelanoma activity. *Proc Natl Acad Sci USA* 105:3041–3046. <https://doi.org/10.1073/pnas.0711741105>
148. Cox JR, Woodcock Stephen, Hillier IH, Vincent MA (1990) Tautomerism of 1,2,3- and 1,2,4-triazole in the gas phase and in aqueous solution: a combined ab initio quantum mechanics and free energy perturbation study. *J Phys Chem* 94:5499–5501. <https://doi.org/10.1021/j100377a016>